Universiteit
Leiden
The Netherlands

Combined Mcl-1 and YAP1/TAZ inhibition for treatment of metastatic uveal melanoma

Glinkina, K.A.; Teunisse, A.F.A.S.; Gelmi, M.C.; Vries, J. de; Jager, M.J.; Jochemsen, A.G.

Combined Mcl-1 and YAP1/TAZ inhibition for treatment of metastatic uveal melanoma

Kseniya A. Glinkina[a], Amina F.A.S. Teunisse[a], Maria Chiara Gelmi[b], Jelle de Vries[a], Martine J. Jager[b] and Aart G. Jochemsen[a]

Uveal melanoma is the most common intraocular tumor in adults, representing approximately 5% of all melanoma cases. Up to 50% of uveal melanoma patients develop metastases that are resistant to most of the commonly used antineoplastic treatments. Virtually all uveal melanoma tumors harbor activating mutations in *GNAQ* or *GNA11*, encoding Gαq and Gα11, respectively. Constant activity of these proteins causes deregulation of multiple downstream signaling pathways including PKC, MAPK and YAP1/TAZ. While the importance of YAP1 signaling for the proliferation of uveal melanoma has recently been demonstrated, much less is known about the paralog of YAP1 transcriptional coactivator, named TAZ; however, similar to YAP1, TAZ is expected to be a therapeutic target in uveal melanoma. We performed a small-scale drug screen to discover a compound synergistically inhibiting uveal melanoma proliferation/survival in combination with YAP1/TAZ inhibition. We found that the combination of genetic depletion of YAP1/TAZ together with Mcl-1 inhibition demonstrates a synergistic inhibitory effect on the viability of uveal melanoma cell lines. Similarly, indirect attenuation of the YAP1/TAZ signaling pathway with an inhibitor of the mevalonate pathway, that is, the geranyl-geranyl transferase inhibitor GGTI-298, synergizes with Mcl-1 inhibition. This combination could be potentially used as a treatment for metastatic uveal melanoma. *Melanoma Res* 33: 345–356 Copyright © 2023 The Author(s). Published by Wolters Kluwer Health, Inc.

Introduction

Uveal melanoma is an intraocular tumor arising from the melanocytes located in the choroid, iris or ciliary body [1,2]. Despite the effectiveness of local therapies, approximately half of the uveal melanoma patients develop distant metastases, which most often target the liver [3]. As aggressive uveal melanoma metastases demonstrate resistance to most of the commonly used antineoplastic drugs, the median survival after diagnosis does not reach 1 year [4].

Recently the first therapeutic agent, tebentafusp, has been approved by the Federal Drug Administration for the treatment of metastatic uveal melanoma. Tebentafusp is a bi-specific protein that binds the gp100-HLA-A*02 : 01 protein on uveal melanoma cells and CD3 on the T-cell membrane, thereby redirecting the T cells towards uveal melanoma cells. Overall survival at 1 year was 73% in the tebentafusp group and 59% in the control group [5];

however, only HLA-A*02 : 01-positive patients can benefit from this treatment approach. The more widely used immunotherapeutics, such as the checkpoint inhibitors anti-CTLA4 and anti-PDL1, have not shown promising results except for patients with tumors that express no MBD4 [6–8]

In general, therapeutic options for metastatic uveal melanoma remain very limited [9]. Chemotherapeutics such as fotemustine or dacarbazine failed to increase overall survival [10,11], and targeted drugs designed for the treatment of metastatic cutaneous melanoma are not beneficial for uveal melanoma patients, because these melanoma subtypes have a distinct genetic profile.

The characteristic feature of uveal melanoma is the constant activation of Gα-protein signaling. Activating mutations frequently occur in the *GNAQ* and *GNA11* genes, encoding the Gα protein subunits Gαq and Gα11, respectively (93% of uveal melanoma); less common are mutations in the G-protein coupled receptor *CYSLTR2* and the signal mediator *PLCB4* [12–14]. The mutated Gα subunit lacks its intrinsic GTPase activity and remains in the activated, GTP-bound state, even in the absence of external stimuli. It permanently activates PLCβ, which cleaves phosphatidylinositol bisphosphate into diacylglycerol and inositol triphosphate and mediates

subsequent activation of PKC and the MAPK pathway [15,16]. Inhibition of both PKC and MEK is required in order to control uveal melanoma growth, as follows from preclinical studies [15]. PKC inhibitors AEB071 (Sotrastaurin) and LXS196 (Darovasertib) demonstrated clinical activity, but limited efficacy during phase I clinical trials [17,18]. The phase Ib trial of the combination AEB071 and MEK inhibitor MEK162 (Binimatinib) has not been completed due to strong adverse effects and a low response (NCT01801358).

Independently of PLCβ, mutated Gαq activates other small G-proteins, RhoA and Rac1, via the nucleotide exchange factor Trio. Remarkably, mutated Gαq, but not the wild-type protein, has been shown to form a stable complex with Trio [19]. In turn, GTP-bound RhoA, via several downstream effectors, induces the accumulation of F-actin which displaces the transcription coactivator YAP1 from its complex with AMOT. This released YAP1 may translocate to the nucleus, interact with DNA-bound cofactors like TEAD or AP-1 and start YAP1-dependent transcription [20,21].

The mevalonate pathway is another signaling route that can lead to the activation of RhoA and Rac1 with the consequential activation of YAP1/TAZ. Mechanistically, the mevalonate reaction cascade results in the production of geranyl-geranyl pyrophosphate, an isoprenoid molecule that serves as a posttranslational modification of Rho GTPases. Geranyl-geranylation of RhoA (and Rac1) is essential for its localization to the cellular membrane and activation. Active RhoA inhibits the phosphorylation of YAP1 on Ser127 and promotes its shuttling into the nucleus [22].

Recently, the tyrosine kinase FAK has been reported to play a role downstream of Trio-RhoA in the activation of YAP1 activity, and targeting FAK has been suggested as a therapeutic option for uveal melanoma metastases [20].

YAP1 and structurally related to its transcriptional coactivator TAZ regulate numerous cellular processes such as cytoskeleton remodeling, cell polarity and proliferation [23–25]. Active YAP1 signaling has been reported to play a role in the malignant transformation of uveal melanocytes [26,27]. Interference with YAP1/TAZ activity is considered a therapeutic option for several types of cancer, and the search for effective inhibitors is ongoing [28–30].

In uveal melanoma, control of YAP1 signaling with verteporfin, a compound that blocks the interaction of YAP1 with the cofactors TEAD, has been shown to slow down cell proliferation and tumor formation *in vivo* [21,31]. Recent reports, however, question the previously demonstrated effects of YAP1 on proliferation of uveal melanoma cells and on patient survival [32,33]. Interestingly, Wang *et al*. show a significant correlation between *WWTR1* (encoding TAZ), but not *YAP1* mRNA expression and uveal melanoma patient survival [34]. The study of Brouwer *et al*. demonstrated the correlation between

high expression of YAP1 and TAZ and the risk of developing uveal melanoma metastases [35].

We show here that depletion of TAZ is synergistic with inhibition of Mcl-1 in reducing uveal melanoma cell survival. Mcl-1 (Myeloid leukemia 1) is an antiapoptotic protein of the Bcl-2 family, which prevents apoptosis by binding to the pro-apoptotic members of Bcl-2 family [36]. Mcl-1 is overexpressed in various tumor types and has been found responsible for antineoplastic drug resistance, which makes it an attractive therapeutic target [37–40]. Several Mcl-1 inhibitors, including MIK665 and AZD5991 utilized in our experiments, have entered clinical trials [36,41].

YAP1/TAZ activity can be repressed by an inhibitor of geranylgeranyl-transferase, an intermediate in the mevalonate pathway, for example, GGTI-298 [22]. Combining GGTI-298 with inhibition of Mcl-1 also synergistically inhibits survival and induces apoptosis in uveal melanoma cells. Similarly, the recently described inhibitor of the palmitoylation of TEADs, K-975, affects YAP1/TAZ activity, uveal melanoma proliferation and synergizes with Mcl-1 inhibition.

Methods

Cell culture

Cell lines OMM2.5, OMM2.3, MEL285, MEL290, (a gift of Dr. B.R. Ksander, Schepens Eye Research Institute, Boston, Massachusetts, USA) [42,43] and OMM1 [a gift of Dr. Gré Luyten, Leiden University Medical Centre (LUMC), Leiden, the Netherlands] [44], were cultured in a mixture of RPMI and DMEM-F12 (1 : 1) supplemented with 10% FBS and antibiotics. MM28, MP38, MP46 and MM66 [45] were cultured in IMDM supplemented with 20% FBS and antibiotics. The cell lines were maintained in a humidified incubator at 37 °C with 5% CO_2.

Generation of cell lines with inducible knockdown of *YAP1* and *WWTR1*

The inducible short hairpin RNA (shRNA) knockdown lentiviral vectors were constructed as described by Herold *et al* [46]. Lentiviral particles were produced by transfecting HEK293T cells seeded in 15-cm dishes with 13.7 μg of vector DNA together with three helper plasmids (11.4 μg of pMDL-RRE, 5.4 μg of pRSV-REV and 7.5 μg of pVSV-G) mixed with 114 μg of polyethylenimine. The virus-containing cell culture supernatants were collected 48 h after transfection and passed through a 0.45-μm filter. The virus titer was quantified by ELISA, measuring HIV p24 levels (ZeptoMetrix Corp., New York, New York, USA). The cells (OMM1 and OMM2.5) were transduced with lentiviruses with multiplicity of infection = 2 in a medium containing 8 μg/ml polybrene. The shRNA target sequences to deplete *YAP1* and *WWTR1* and the control sequence are shown in Supplementary Table 1, Supplemental digital content 1, *http://links.lww.com/MR/A345*.

Table 1   Drugs included in the screen

Drug	Target/Mechanism of action	Reference
Silmitasertib	Casein Kinase 2, Cyclin-like kinases	[49]
RG7112	MDM2-p53 interaction/ p53 activator	[50]
Nutlin-3	MDM2-p53 interaction/ p53 activator	[51]
Sotrastaurin	Protein kinase C	[16]
Everolimus	mTORC1	[52]
KU0063794	mTORC1/2	[53]
Ribociclib	Cyclin-dependent kinase 4/6	[54]
Foretinib	c-Met, VEGFR2, Tyro, Axl, MERTK	[55]
Navitoclax	Bcl-2, Bcl-xL, Bcl-w	[56]
Venetoclax	Bcl-2	[57]
S63845	Mcl-1	[58]
MIK665	Mcl-1	[59]

Compound screen

Cells were seeded in appropriate concentrations in 6 by 6 wells into 96-well plates. The next day, the media in half of the wells was supplemented with 50 ng/ml doxycycline for the 1st round of screening and 10 ng/ml doxycycline for the 2nd round. Next day serial dilutions of inhibitors were added in all the wells. Viability was accessed after 5 days of compound treatment using CellTiter-Blue cell viability assay (Promega, Madison, Wisconsin, USA).

A putative synergistic effect was calculated using Excess-over-Bliss algorithm [47,48].

Everolimus, Foretinib, KU0063794, Ribociclib, Silmitasertib, Sotrastaurin and RG7112 were obtained from Selleck Chemicals (Houston, Texas, USA), Navitoclax, MIK665 and S63845 from MedChem Express (Monmouth Junction, New Jersey, USA), Nutlin-3 from Cayman Chemical (Ann Arbor, Michigan, USA) and Venetoclax from Torcis Bioscience (Abingdon, UK) The targets of the inhibitors are listed in Table 1.

Cell viability assay

The cells were seeded at their appropriate concentrations into clear 96-well plates. The next day, the medium was supplemented either with 20 ng/ml doxycycline or/and with a compound. The treatment was repeated after 2 days. After 5 days (in case of doxycycline treatment) or 3 days from beginning of the experiment, the viability of the cells was assessed using the CellTiter-Blue cell viability assay (Promega).

Caspase 3/7 activity

The cells were seeded in triplicate into white-walled 96-well plates with clear bottoms or in clear 96-well plates. The next day, the media was supplemented with doxycycline 20 ng/ml (OMM1) or 40 ng/ml (OMM2.5) and a compound. After 3 days of treatment, the caspase 3/7 activity was assessed with the use of the Caspase-Glo 3/7 assay (Promega) and cell viability was assessed with the CellTiter-Blue assay (Promega). Caspase activity relative to viability was calculated.

Western blot

The cells were seeded into 6-well plates. The next day the media were supplemented with solutions containing doxycycline, Mcl1-inhibitor MIK665 or a combination of both. After 3 days, the cells were rinsed two times with ice-cold Phosphate Buffered Saline and scraped and lysed with Giordano buffer (50 mM Tris-HCl pH = 7.4, 250 mM NaCl, 0.1% Triton X-100, 5 mM EDTA, supplemented with phosphatase- and protease inhibitors. Equal protein amounts were separated on SDS-PAGE and blotted on PVDF membranes (Millipore, Darmstadt, Germany). The membranes were blocked with 10% nonfat dry milk in TBST buffer (10 mM Tris-HCl pH = 8.0, 150 mM NaCl, 0.2% Tween-20) and incubated with the primary antibodies diluted in 5% BSA/TBST overnight at 4 °C. The membranes were washed with TBST and incubated with horseradish peroxidase-conjugated secondary antibodies (Jackson Laboratories, Bar Harbor, Maine, USA). The chemiluminescent signal was visualized using a Chemidoc machine (Bio-Rad, Hercules, CA, USA). The bands were quantified using ImageLab software (Bio-Rad).

Primary antibodies against YAP1 (D8H1X), TAZ (V386) and PARP (#9542) were obtained from Cell Signaling Technology, Beverly, Massachusetts, USA; against Vinculin (V9131) from Sigma-Aldrich (St Louis, Missouri, USA).

RNA isolation and quantitative PCR

The cells were seeded into 6-well plates. The next day, media were supplemented with either doxycycline (40 ng/ml for OMM2.5, 20 ng/ml for OMM1) or/and a compound. After 3 days of treatment, cells were collected by scraping and placed in lysis buffer and RNA was isolated using the SV Total RNA Isolation System (Promega) according to the manufacturer's protocol. The reverse transcription reaction was performed using ImPromII reverse transcriptase (Promega). qPCR was performed using SYBR Green Mix (Roche Diagnostics, Indianapolis, Indiana, USA) in a C1000 Touch Thermal Cycler (Bio-Rad laboratories). The relative expression of target genes was determined and corrected in relation to the housekeeping genes *CAPNS1* and *SRPR*. In each experiment, the average relative expression was compared to the untreated, set at 1. Primer sequences are listed in Supplementary Table 2, Supplemental digital content 1, *http://links.lww.com/MR/A345*.

Statistical analysis

The data were analyzed using GraphPad Prism software v.9.1.0 (GraphPad Software, San Diego, California, USA). Student's *t*-test was used to analyze the difference between the two groups. One-way analysis of variance was used to analyze the differences between multiple groups. *P* values of 0.05 or less were considered significant.

Clinical data analysis

The LUMC cohort includes clinical, histopathological and genetic information on 64 cases treated with primary enucleation at the LUMC between 1999 and 2008. Clinical information was collected from the Integral Cancer Center West patient records and updated in 2021.

After enucleation, part of the tumor was snap-frozen with 2-methyl butane and used for mRNA and DNA isolation, while the remainder was embedded in paraffin after 48 h of fixation in 4% neutrally buffered formalin and was sent for histological analysis. RNA was isolated with the RNeasy mini kit (Qiagen, Venlo, The Netherlands), and mRNA expression was determined with the HT-12 v4 chip (Illumina, San Diego, California, USA). Chromosome 3 status was obtained with single-nucleotide polymorphism analysis, performed with the Affymetrix 250K_NSP-chip and Affymetrix Cytoscan HD chip (Affymetrix, Santa Clara, California, USA).

The Cancer Genome Atlas (TCGA) cohort represents 80 primary uveal melanoma cases enucleated in six different centers [14]. mRNA expression was determined by RNA-seq.

The statistical software SPSS, version 25 (IBM Corp, Armonk, New York, USA) was used for statistical analyses of the LUMC and TCGA cohorts. Survival analysis was performed with Kaplan–Meier and log-rank test, with death due to metastases as an endpoint. Cases that died of another or unknown cause were censored. The two subpopulations that were compared in each analysis were determined by splitting the total cohort along the median value of mRNA expression for the analyzed gene.

The study was approved by the Biobank Committee of the Leiden University Medical Center (LUMC; 19.062. CBO/uveamelanoomlab-2019-3; B20.023). The tenets of the Declaration of Helsinki were followed.

Synthesis and structure analysis of K-975

General reagents and solvents were purchased from Sigma-Aldrich, Biosolve (Valkenswaard, the Netherlands) and VWR (Amsterdam, the Netherlands) and used as received. 3-(4-chlorophenoxy)-4-methylaniline (CAS number 1400872-19-6, article number EN300-7432581) was purchased from Enamine (Riga, Latvia) and used as received.

Reactions were performed under an inert nitrogen atmosphere. 3-(4-chlorophenoxy)-4-methylaniline (50 mg; 0.21 mmol) was taken up in dichloromethane (5 ml). Triethylamine (89 µl; 0.64 mmol) was added and the mixture was stirred for a few minutes before addition of acryloyl chloride (19 µl; 0.23 mmol). The mixture was stirred at room temperature and progress was monitored by thin-layer chromatography (TLC) analysis.

TLC analysis was performed on Merck aluminum sheets (precoated with silica gel 60 F254; Merck KgaA Darmstadt, Germany). Compounds were visualized by ultraviolet (UV) absorption (254 nm) and by using a solution of ninhydrin (15 g l^{-1}) in 3% AcOH/EtOH v/v.

Upon completion, the crude reaction mixture was adsorbed onto Celite for purification. Compounds were purified on a Büchi Sepacore (Hendrik-Ido-Ambacht, the Netherlands) automatic flash chromatography system X10/X50 using an ethyl acetate – heptane gradient. The Büchi Sepacore system was equipped with two Büchi pump modules C-605, a Büchi control unit C-620, a Büchi fraction collector C-660 and a Büchi UV Photometer C-640. The silica columns were purchased at GraceResolv and were packed with a grade of Davisil silica.

The pure fractions were combined and concentrated to dryness *in vacuo* at 40 °C followed by lyophilization from an acetonitrile–water mixture to give the desired product as a yellow solid (44 mg; 0.15 mmol; 73%).

NMR spectra (^{1}H, ^{13}C) were recorded on a Bruker (Fällanden, Switzerland) Ultrashield 300 MHz spectrometer at 298 K (Supplementary Fig. 1 A, B, Supplemental digital content 2, *http://links.lww.com/MR/A346*).

Liquid chromatography-mass spectrometry (LC-MS) measurements were performed on an LC-MS system equipped with a Waters (Etten-Leur, the Netherlands) Acquity H-Class UPLC system with an Extended λ Photodiode Array Detector (210–800 nm), an Acquity BEH C18 Column (130 Å, 1.7 µm, 2.1 mm × 50 mm) and an LCT-Premier ESI-Orthogonal Acceleration Time of Flight Mass Spectrometer. Samples were run using three mobile phases: A = Purified deionized Water (Veolia – H_2O), B = Acetonitrile (UPLC grade – CH_3CN) and C = 44% H_2O, 44% CH_3CN, 12% Formic acid (UPLC grade – HCO_2H). Data processing was performed using Waters MassLynx Mass Spectrometry Software 4.1. UPLC-MS Program: flow rate = 0.5 ml/min, runtime = 3 min, column T = 40 °C, mass detection: 100–1500 Da. Gradient: Line C, provides a constant 4% of the total composition. Initial conditions 94% A, 2% B, 4% C at 0.2 min. Composition gradually changes over 1.6 min, to 96% B and 4% C at 1.80 min. This is kept until 2.15 min before changing back to the original composition at 2.20 min and remains so until the 3 min time mark. The spectra are shown in Supplementary Fig. 1 C, Supplemental digital content 2, *http://links.lww.com/MR/A346*.

Results

Depletion of TAZ sensitizes uveal melanoma cells to inhibition of Mcl-1

In order to study the function of YAP1 and TAZ in metastatic uveal melanoma, we generated derivatives of the

metastasis-derived uveal melanoma cell lines OMM2.5 and OMM1, containing doxycycline-inducible shRNAs targeting *YAP1* (i-shYAP), *WWTR1* (i-shTAZ) or both (i-shYAP/TAZ) and non-targeting controls (i-shCtrl and i-shCtrl/Ctrl). The efficiency of the knockdown can be observed in Supplementary Fig. 2 A-B, Supplemental digital content 3, *http://links.lww.com/MR/A347*. Induction of shRNA expression with doxycycline led to substantial depletion of the respective proteins, without any effect on the control cells. The residual level of YAP1 protein varied between the distinct i-shYAP-containing cell lines: the knockdown by the i-shYAP#2 (80% protein depletion in OMM2.5 and 90% in OMM1) was more efficient than i-shYAP#1 (70% in both cell lines).

In OMM2.5 cells, the knockdown of TAZ significantly reduced the expression of the canonical YAP1/TAZ target genes *CTGF* and *CYR61*, while the depletion of YAP1 had no or little effect (Supplementary Fig. 2 C B, Supplemental digital content 3, *http://links.lww.com/MR/A347*). In OMM1 cells, the expression of *CTGF* was downregulated upon YAP1 or TAZ knockdown, but only depletion of TAZ reduced the level of *CYR61* mRNA (Supplementary Fig. 2 D B, Supplemental digital content 3, *http://links.lww.com/MR/A347*). In both cell lines, the effect of the double YAP1/TAZ knockdown on transcription of the target genes was greater than TAZ knockdown alone, suggesting that YAP1 might to some extent compensate for the effect TAZ depletion has on the tested targets.

Depletion of TAZ significantly inhibited the growth of both tested cell lines (Supplementary Fig. 2 E-F B, Supplemental digital content 3, *http://links.lww.com/MR/A347*). Expression of i-shYAP#1 hardly affected cell growth, but the induced expression of i-shYAP#2 could slow down the growth of the cells to the same extent as i-shWWTR1, which is possibly explained by the less efficient depletion of YAP1 in i-shYAP#1 cells. Simultaneous knockdown of YAP1 and TAZ caused slightly stronger inhibition of cell growth, compared to either of the single knockdowns.

Because depletion of YAP1 and TAZ slows down the proliferation of uveal melanoma cells, these transcriptional coactivators can be considered as putative therapeutic targets in uveal melanoma; however, as knockdown of YAP1 and TAZ does not cause apoptosis, as illustrated by little PARP cleavage upon treatment with doxycycline in Supplementary Fig. 2 A-B, B, Supplemental digital content 3, *http://links.lww.com/MR/A347* the cells may quickly develop resistance to their inhibition. Therefore, we performed a small-scale drug screen in order to find a therapeutic target, which upon simultaneous inhibition with YAP1 or TAZ depletion would force the uveal melanoma cells into apoptosis. We treated OMM2.5/i-shYAP#2,/i-shTAZ#1 and/i-shCtrl with serial dilutions of various compounds developed to target cancer cells (Table 1),

in the absence or presence of doxycycline. On the basis of the obtained dose-response curves, we calculated the synergistic score using the Excess-over-Bliss (EoB) algorithm. A positive EoB value indicates synergism between two compounds, values close to zero refer to an additive effect, negative values indicate antagonism. The calculated best EoB values for the tested drugs are summarized in Fig. 1a. The two inhibitors of Mcl-1, S63845 and MIK665, both demonstrated very good synergism with depletion of both YAP1 and TAZ, as well as the Bcl-2/Bcl-xl/Bcl-w inhibitor Navitoclax; the selective Bcl-2 inhibitor Venetoclax was synergistic only with depletion of TAZ, but not YAP1. Overall, the result of the screen highlights that inhibitors of Bcl-2 family members, such as Bcl-2 and Mcl-1, can be synergistic with inhibition of YAP1 or TAZ.

Remarkably, OMM2.5 was very sensitive to the Mcl-1 inhibitors with IC50s in the low nanomolar range, while survival of OMM1 cells was inhibited only by low micromolar concentrations (Supplementary Fig. 3 A, Supplemental digital content 4, *http://links.lww.com/MR/A348*). This difference could not be explained by a distinct expression level of Mcl-1 between these cell lines (data not shown).

The enhanced sensitivity of the TAZ-depleted uveal melanoma cells to Mcl-1 inhibition is illustrated in Fig. 1b and c and Supplementary Fig. 3 B, Supplemental digital content 4, *http://links.lww.com/MR/A348*. OMM2.5 and OMM1 with doxycycline-induced knockdown of TAZ were more sensitive to Mcl-1 inhibitors after 3 days of treatment: in OMM2.5, induction of i-shYAP#2 sensitized the cells to MIK665, but in OMM1 cells, depletion of YAP1 did not have any effect on MIK665 sensitivity. The effect of YAP1/TAZ double knockdown was slightly more pronounced than TAZ knockdown in both cell lines. This reduction of cell viability was most likely a result of increased apoptosis, as suggested by the elevated activity of caspases 3 and 7 (Fig. 1d and e and Supplementary Fig. 3 C, Supplemental digital content 4, *http://links.lww.com/MR/A348*). The activated caspases cleave PARP protein and cleaved PARP serves as a marker of apoptosis. The band of cleaved PARP in the MIK665-treated derivatives of OMM2.5 was detected by western blot, as shown in Supplementary Fig. 2 A B, Supplemental digital content 3, *http://links.lww.com/MR/A347*. The signal became stronger with addition of doxycycline in i-shTAZ and i-shYAP#2, together with disappearance of the band of full-length PARP, which supports the induction of apoptosis of uveal melanoma cells upon simultaneous inhibition of TAZ and Mcl-1. This effect was even stronger in the double YAP1/TAZ knockdown. In OMM1/i-shYAP or/i-shTAZ cells, the band of cleaved PARP was hardly visible but was clearly detected in the double knockdown cell lines upon treatment with doxycycline and the combination of doxycycline and MIK665 (Supplementary Fig. 2 B

Fig. 1
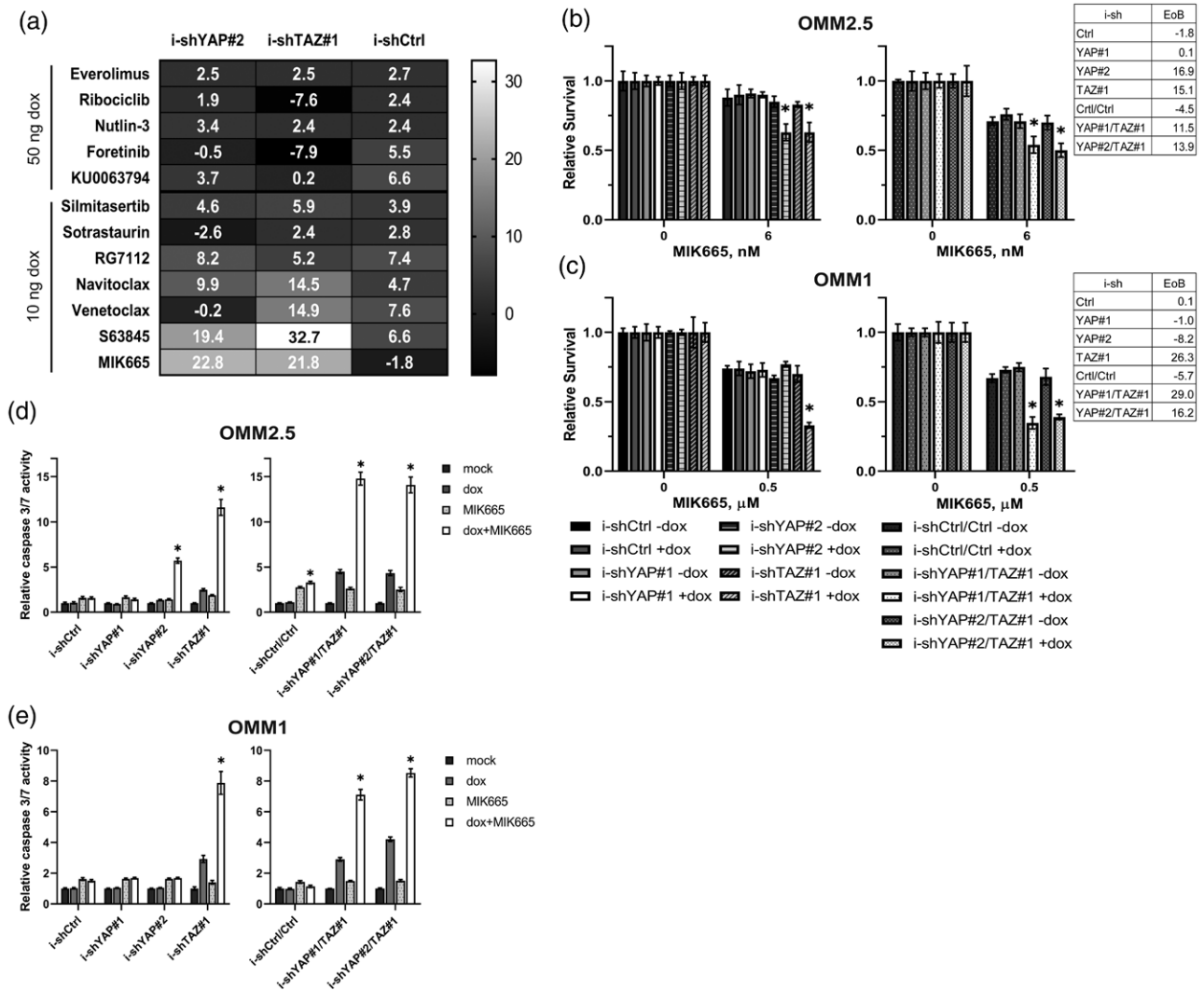
YAP1/TAZ depletion synergizes with Mcl-1 inhibitors in growth inhibition and apoptosis induction in uveal melanoma cell lines. (a) The matrix of the highest Excess-over-Bliss (EoB) synergy scores of each treatment per knockdown cell line. (b) OMM2.5 or (c) OMM1 cells containing either i-shControl or i-shYAP vectors, or i-shTAZ, or both i-shYAP/TAZ vectors were seeded into 96-well plates; the next day the medium was supplemented with doxycycline (+dox) (OMM2.5 : 40 ng/ml, OMM1 : 20 ng/ml) and with MIK665. The treatment was refreshed every other day, the plates were analyzed after 5 days. The plots represent the averages normalized to respective samples not treated with MIK665, error bars present mean ± SEM. Significant reduction ($P < 0.05$) of viability in +dox compared to -dox upon MIK665 treatment is indicated with (*), statistical analysis was performed using t-test, (d and e) Induction of apoptosis in (d) OMM2.5 and (e) OMM1 cell lines upon treatment with doxycycline (OMM2.5 : 40 ng/ml, OMM1 : 20 ng/ml) and MIK665 (OMM2.5 : 6 nM, OMM1 : 0.5 µM) for 3 days. Activity of caspases 3/7 was measured after 5 days of treatment; significant ($P < 0.05$) elevation of caspases 3/7 activity in combinational treatment comparing to both of the single treatments is indicated with (*), statistical analysis was performed using one-way ANOVA, error bars present mean ± SEM. ANOVA, analysis of variance.

B, Supplemental digital content 3, *http://links.lww.com/MR/A347*).

To find an explanation for the increased apoptosis, we analyzed the mRNA expression of several apoptosis regulatory proteins, including *Bcl-2*, *Mcl1*, *Bim*, *BMF*, *Noxa* and *Survivin*.

Expression of most of these genes was not consistently affected upon doxycycline, MIK665 or combination treatment (data not shown); however, in the TAZ knockdown and the double-knockdown cells, *Bcl-2* expression was significantly downregulated in the cells treated with doxycycline + MIK665 (Fig. 2a) compared to both single treatments. Induction of i-shYAP#2 with doxycycline decreased *Bcl-2* expression compared to a control, but treatment with MIK665 did not significantly enhance this effect.

Inhibition of Mevalonate pathway allows indirect control of YAP and TAZ activity

It has been shown before that inhibition of geranyl-geranyl transferase, which is important for the activation

of RhoA/Rac1, indirectly blocks the activation of YAP1 and TAZ [22]. Therefore, we used the geranyl-geranyl transferase inhibitor GGTI-298 to investigate its effect together with Mcl-1 inhibition on expression of YAP1/TAZ target genes, YAP1, TAZ and Mcl-1 protein levels and uveal melanoma proliferation/survival.

Several uveal melanoma cell lines treated with GGTI-298 demonstrated strong downregulation of expression of the YAP1/TAZ transcription targets *CTGF* and *CYR61*, as well as *FOXM1* and *Survivin* (Fig. 2b). At the protein level, we noticed a slight downregulation of YAP1 and TAZ after treatment with GGTI-298 in OMM2.3 and MP46 cells (Fig. 2c and Supplementary Fig. 3 D, Supplemental digital content 4, *http://links.lww.com/MR/A348*). Treatment with the Mcl-1 inhibitors MIK665 (Fig. 2c) or S63845 (Supplementary Fig. 3 D, Supplemental digital content 4, *http://links.lww.com/MR/A348*) did not change the levels of YAP1 (except MP38 and OMM2.3 cells) and TAZ, but caused elevation in the level of Mcl-1. In the subset of samples treated with the combination of GGTI-298 and Mcl-1 inhibitor, we see a slightly further downregulation of YAP1 and TAZ, compared to mono treatment with GGTI-298. The intensity of the Mcl-1 band in the samples treated with the combination remains similar to the band in the samples treated with only Mcl-1 inhibitors (in OMM1 and OMM2.3) or slightly decreases in MP38 and MP46.

Next, we assessed the effect of the combination GGTI-298 with MIK665 on the survival of uveal melanoma cell lines. In all of the cases, the combination reduced the survival of the cells more strongly than either of the single treatments (Fig. 2d) and the positive EoB scores indicated synergism. Interestingly, the synergistic effect was not demonstrated in MEL285 and MEL290, uveal melanoma cell lines that do not contain activating mutations in GNAQ or GNA11 (Supplementary Fig. 4 A, Supplemental digital content 5, *http://links.lww.com/MR/A349*). The combination of GGTI-298 and MIK665 increased the activity of caspases 3/7 in most of the tested cell lines, except for OMM1, MEL285, MEL290 (Fig. 2e and Supplementary Fig. 4 B, Supplemental digital content 5, *http://links.lww.com/MR/A349*).

Recently the results of Phase 1 clinical trial with another geranyl-geranyl transferase inhibitor, that is, GGTI-2418, were published [60]. Therefore, we tested also GGTI-2418 in combination with MIK665 on some uveal melanoma cell lines (Supplementary Fig. 4 C, Supplemental digital content 5, *http://links.lww.com/MR/A349*). In line with the original publication using this inhibitor on cell lines in culture, much higher concentrations of this compound were needed to affect the growth of uveal melanoma cell lines, and even treatment with 40 μM demonstrated only a limited effect. Even so, some synergism with MIK665 was found although not as good as GGTI-298.

To verify that the observed synergistic effect of simultaneous blocking of TAZ signaling and Mcl-1 was not restricted to an Mcl-1 inhibitor of a particular molecular structure, we also tested AZD5991, an Mcl-1 inhibitor structurally distinct from MIK665 and S63845 [61]. The uveal melanoma cells were less sensitive to AZD5991 than to MIK665, as higher concentrations of AZD5991 were required to get comparable growth inhibition. The combination of GGTI-298 with AZD5991 demonstrated a synergistic effect in most of the tested uveal melanoma cell lines, confirming the effect seen with MIK665 and S63845, although the EoB values were lower than in combination with MIK665 (Supplementary Fig. 4 D, Supplemental digital content 5, *http://links.lww.com/MR/A349*).

Direct inhibition of the YAP1/TAZ-TEAD interaction with K-975

The inhibition of the mevalonate pathway with GGTI-298 diminishes YAP1- and TAZ-mediated transcription activation but, because the effect on YAP/TAZ via RhoA inactivation is indirect, it likely interferes with multiple cellular processes apart from YAP1 and TAZ activity. To investigate more directly the functions of the YAP1/TEAD and TAZ/TEAD transcription complexes in uveal melanoma, we employed a recently described compound, K-975, which covalently interacts with an internal cysteine residue located in the palmitate-binding pocket of TEADs. Because palmitoylation of this cysteine stabilizes the TEAD proteins and is required for the interaction with YAP1 or TAZ [62,63], K-975 treatment results in the inhibition of these interactions and downregulation of expression of YAP1/TAZ target genes in mesothelioma cell lines [64]. Likewise, treatment of uveal melanoma cell lines with K-975 significantly reduced the mRNA expression of the tested YAP1/TAZ target genes (Fig. 3a). The growth of all tested uveal melanoma cell lines was inhibited by K-975 treatment, although OMM2.3 and OMM2.5 were relatively insensitive (Fig. 3b). Similar to the results obtained with GGTI-298, combining K-975 with MIK665 synergistically enhanced the growth reduction in uveal melanoma cells except MP46 cells (Fig. 3c). Increase in caspase 3/7 activity upon treatment with K-975-MIK665 combination varied per cell line: OMM1 demonstrated no elevation, while MP38 showed a more than four-fold increase (Fig. 3d).

Analysis of clinical data

The correlation of YAP1/TAZ expression with the survival of uveal melanoma patients has been discussed previously [33,35]. Having demonstrated the synergistic effect of the combination of YAP1/TAZ and Mcl-1 on the proliferation of uveal melanoma cells, we decided to examine if the expression of Mcl-1 could be related to the metastatic potential of uveal melanoma and survival of metastatic uveal melanoma patients. We analyzed

Fig. 2
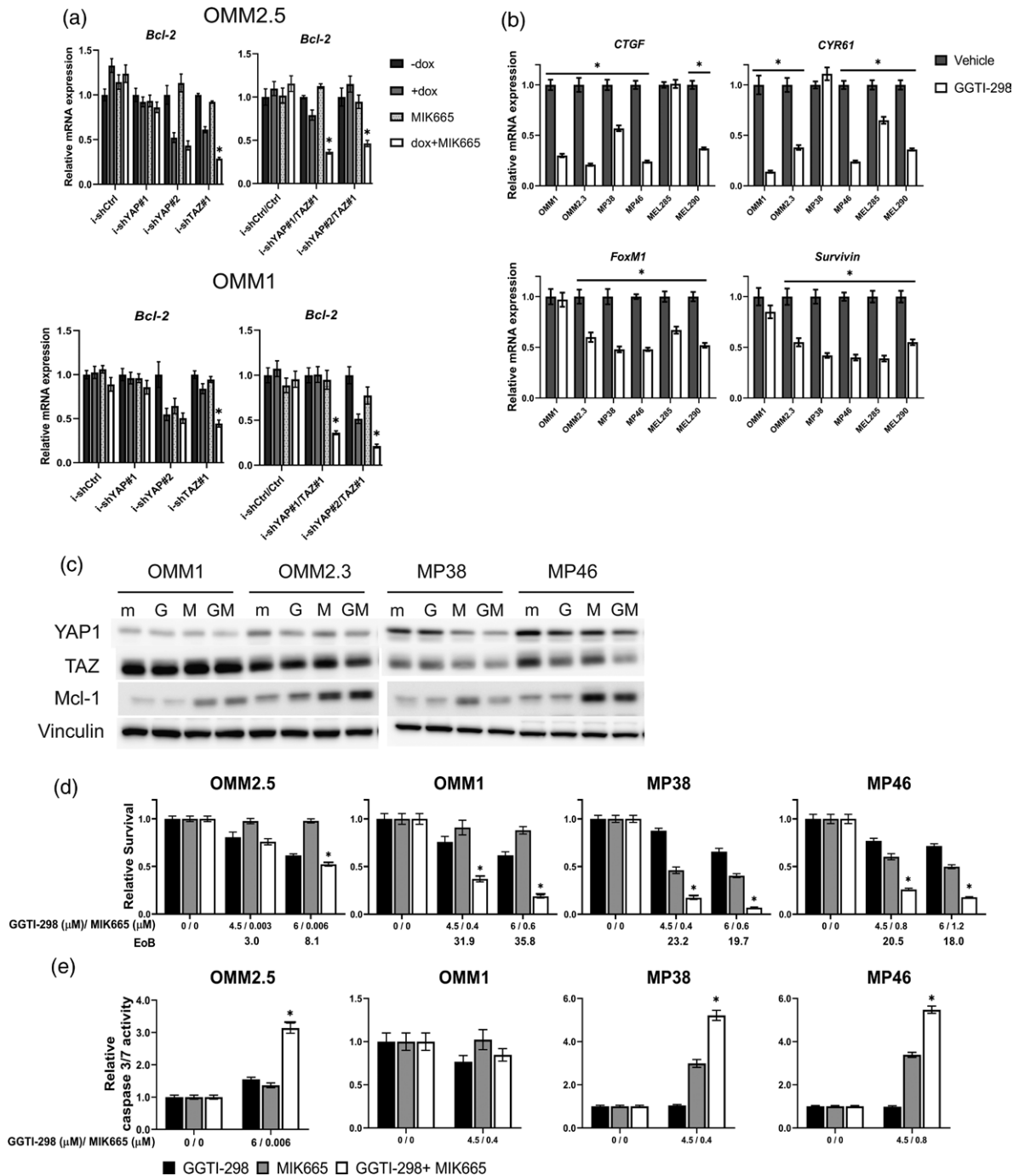
GGTI-298 indirectly inhibits YAP1/TAZ signaling and synergizes with Mcl-1 inhibition. (a) Expression of *Bcl-2* mRNA upon 24 h treatments with dox-ycycline (OMM2.5 : 40 ng/ml, OMM1 : 20 ng/ml), MIK665 (OMM2.5 : 6 nM, OMM1 : 0.5 μM), or the combination. Significant ($P < 0.05$) change in mRNA expression of the combination compared to both of the single treatments is indicated with (*), statistical analysis was performed using one-way ANOVA and error bars present mean ± SEM. (b) Expression of mRNA of YAP1/TAZ target genes upon 24 h treatments with vehicle or GGTI-298 (6 μM), in uveal melanoma cell lines. Significant ($P < 0.05$) change in mRNA expression of the GGTI-298 treated versus vehicle-treated group is indicated with (*), statistical analysis was performed using *t*-test, error bars present mean ± SEM. (c) The effect of GGTI-298 (G; 4 μM), MIK665 (M; OMM1 : 0.2 μM, MP38 : 0.2 μM, OMM2.3 : 6 nM, MP46 : 0.4 μM) or the combination (GM) treatment for 3 days on protein expression of YAP1, TAZ and Mcl-1. Vinculin was used as a loading control. (d) The effect of GGTI-298, MIK665 and their combination on viability of OMM2.5, OMM1, MP38 and MP46 cells after 3 days of treatment. Significant ($P < 0.05$) reduction of viability in combinational treatment compared to both of the single treatments is indicated with (*), statistical analysis was performed using one-way ANOVA, error bars present mean ± SEM. (e) The effect of GGTI-298, MIK665 and their combination on caspase 3/7 activity in OMM2.5, OMM1, MP38 and MP46 cells after 3 days of treatment. Significant ($P < 0.05$) reduction of viability in combinational treatment compared to both of the single treatments is indicated with (*), statistical analysis was performed using one-way ANOVA, error bars present mean ± SEM. ANOVA, analysis of variance.

Fig. 3
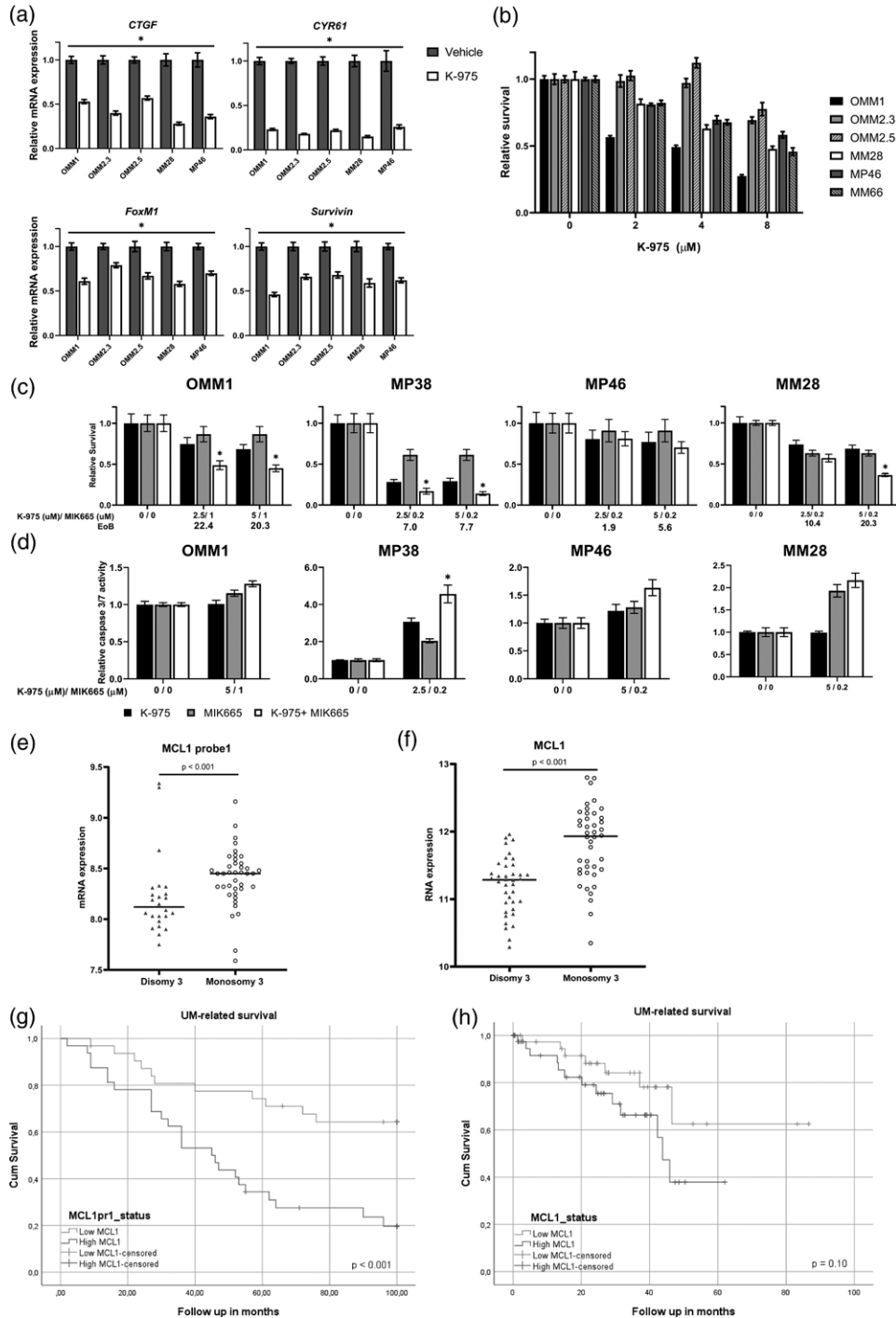
K-975 has an effect on YAP1/TAZ signaling and synergizes with Mcl-1 inhibition (a) Expression of YAP1/TAZ target genes' mRNA upon 24 h treatments with vehicle or 8 µM K-975 in uveal melanoma cell lines. Significant ($P < 0.05$) change in mRNA expression of the GGTI-298 treated versus vehicle-treated group is indicated with (*), statistical analysis was performed using *t*-test, error bars present mean ± SEM. (b) Dose response of uveal melanoma cell lines to treatment with K-975. The cell viability has been assessed after 5 days of treatment. (c) The effect of K-975, MIK665 and their combination on viability of OMM1, MP38, MP46 and MM28 cells after 5 days of treatment. Significant ($P < 0.05$) reduction of viability in combinational treatment compared to both of the single treatments is indicated with (*), statistical analysis was performed using one-way ANOVA and error bars present mean ± SEM. (d) The effect of K-975, MIK665 and their combination on caspase 3/7 activity in OMM2.5, OMM1, MP38 and MP46 cells after 3 days of treatment. Significant ($P < 0.05$) reduction of viability in combinational treatment compared to both of the single treatments is indicated with (*), statistical analysis was performed using one-way ANOVA, error bars present mean ± SEM. (e and f) Correlation of *Mcl-1* mRNA expression with chromosome 3 status of the tumors in LUMC cohort (e, $n = 64$) and TCGA cohort (f, $n = 80$). (g and h) Analysis of the uveal melanoma-specific survival of Mcl-1 in LUMC patient cohort (G, $n = 64$) and TCGA patient cohort (h, $n = 80$). ANOVA, analysis of variance; LUMC, Leiden University Medical Centre; TCGA, The Cancer Genome Atlas.

mRNA expression of *Mcl-1* in two cohorts of uveal melanoma patients: the LUMC cohort including 64 cases (Fig. 3e) and the TCGA cohort including 80 cases (Fig. 3f). The mean expression level of *Mcl-1* probe 1 was 8.34 in LUMC cohort. We stratified the cases by the copy number of chromosome 3, as monosomy 3 and subsequent loss of BAP1 expression represents a crucial predisposing factor for the development of metastases. The mRNA expression of *Mcl-1* turned out to be significantly elevated in the tumors harboring monosomy 3 in both cohorts.

The mRNA expression of *Mcl-1* negatively correlated with the survival of uveal melanoma patients in the LUMC cohort, as demonstrated in Fig. 3g. In the TCGA cohort we observed a similar tendency, but the effect was not significant (Fig. 3h).

The correlation of the expression of *Mcl-1* with the chromosome 3 status and the results suggest a role for Mcl-1 activity for metastases development in uveal melanoma patients, but further analysis is needed to clarify the prognostic significance of this marker.

Discussion

Transcriptional coactivators YAP1 and TAZ have emerged as therapeutic targets for uveal melanoma after the demonstration of their role in the malignant transformation of uveal melanocytes [26]. Although YAP1 and TAZ are structurally and functionally related, their roles in cellular processes are not fully redundant [65]. Our results demonstrate that TAZ and YAP1 have partly overlapping, but also distinct functions in uveal melanoma. Depletion of TAZ leads to more slowdown of the growth of uveal melanoma cells than depletion of YAP1, but knockdown of both YAP1 and TAZ inhibits proliferation even more. The growth reduction in these cases is caused by cell cycle arrest, but not apoptosis, which suggests that inhibition of YAP1 and TAZ in uveal melanoma might not be an effective therapy as a single treatment, but could be potent in combination with other drugs. As shown in the results of our small-scale drug screen, inhibition of Bcl-2 family members, particularly Mcl-1, in combination with TAZ or YAP1 depletion, drives uveal melanoma cells into apoptosis. In line with our findings, *Mcl-1* has been revealed as a hit in a screen of genetic interactions of *WWTR1*, and combination of Mcl-1 inhibitor and blocking TAZ with verteporfin dramatically reduced the viability of nonsmall cell lung cancer cell lines [66].

Verteporfin is a commonly used, but certainly not a specific inhibitor of YAP1 and TAZ, that binds these proteins and interferes with the formation of the complexes with the DNA-bound cofactors TEAD. Although mechanistically distinct, the recently described compound K-975 also disrupts YAP1/TAZ-TEAD complexes by binding to TEADs and inhibiting their palmitoylation. The application of these inhibitors does not allow the complete blocking of YAP1 and TAZ signaling, because they form complexes with the other cofactors, such as AP-1 [67], RUNX1/2 [68], PAX3 [69], BRD4 [70] and SMAD [71]. Possibly due to this fact, we observed a more limited effect of compound K-975 on uveal melanoma cell proliferation, in contrast to drastic growth reduction upon TAZ knockdown. Even so, combining K-975 with Mcl-1 inhibitors synergistically reduced cell viability.

TAZ activity can be modulated not only via blocking its interaction with TEADs, but also via targeting upstream regulators, mainly related to the canonical Hippo pathway, including cell surface receptors [72,73], kinases [74,75], mevalonate pathway inhibitors [22] and actin modulators [76]. The regulation of YAP1 and TAZ activity is complex and context-dependent. In uveal melanoma, YAP1 and TAZ have been reported to be activated by mutant Gαq/11 via FAK kinase [20]. Our data suggest that metabolic regulation via the mevalonate pathway occurs in uveal melanoma, as the geranyl-geranyl transferase I inhibitor GGTI-298 reduces mRNA expression of YAP/TAZ target genes and reduces cell viability. Combination of GGTI-298 with the Mcl-1 inhibitors synergistically reduces cell survival and enhances apoptosis of uveal melanoma cell lines. The clinically tested GGTI-2418 is structurally distinct from GGTI-298 and although it inhibits cell growth to a lesser extent than GGTI-298, it still functions synergistically with the Mcl-1 inhibitor MIK665 in growth inhibition of uveal melanoma cell lines.

Expression of *WWTR1*, encoding TAZ, has been reported before to correlate with monosomy 3 and metastases development [35]. We demonstrate here that higher expression of Mcl-1 also correlates with monosomy of chromosome 3, which represents an important progression marker. Indeed, a high expression of *Mcl-1* showed a tendency to correlate with shorter uveal melanoma patient survival. Therefore, we think that in the future, when clinically relevant TAZ inhibitors have been developed, the combined inhibition of Mcl-1 and TAZ is a therapeutic option for metastases in uveal melanoma patients.

Conflicts of interest

There are no conflicts of interest.

References

1 Virgili G, Gatta G, Ciccolallo L, Capocaccia R, Biggeri A, Crocetti E, *et al.*; EUROCARE Working Group. Incidence of uveal melanoma in Europe. *Ophthalmology* 2007; **114**:2309–2315.

2 Jager MJ, Shields CL, Cebulla CM, Abdel-Rahman MH, Grossniklaus HE, Stern MH, *et al.* Uveal melanoma. *Nat Rev Dis Primers* 2020; **6**:24.

3 Koutsandrea C, Moschos MM, Dimissianos M, Georgopoulos G, Ladas I, Apostolopoulos M. Metastasis rates and sites after treatment for choroidal melanoma by proton beam irradiation or by enucleation. *Clin Ophthalmol* 2008; **2**:989–995.

4 Diener-West M, Reynolds SM, Agugliaro DJ, Caldwell R, Cumming K, Earle JD, *et al.*; Collaborative Ocular Melanoma Study Group Report 23. Screening for metastasis from choroidal melanoma: the Collaborative Ocular Melanoma Study Group report 23. *J Clin Oncol* 2004; **22**:2438–2444.

5 Nathan P, Hassel JC, Rutkowski P, Baurain JF, Butler MO, Schlaak M, *et al.* Overall survival benefit with tebentafusp in metastatic uveal melanoma. *New Engl J Med* 2021; **385**:1196–1206.

6 Rodrigues M, Mobuchon L, Houy A, Fievet A, Gardrat S, Barnhill RL, *et al.* Outlier response to anti-PD1 in uveal melanoma reveals germline MBD4 mutations in hypermutated tumors. *Nat Commun* 2018; **9**:1866.

7 Algazi AP, Tsai KK, Shoushtari AN, Munhoz RR, Eroglu Z, Piulats JM, *et al.* Clinical outcomes in metastatic uveal melanoma treated with PD-1 and PD-L1 antibodies. *Cancer-Am Cancer Soc* 2016; **122**:3344–3353.

8 Zimmer L, Vaubel J, Mohr P, Hauschild A, Utikal J, Simon J, *et al.* Phase II DeCOG-study of ipilimumab in pretreated and treatment-naive patients with metastatic uveal melanoma. *PLoS One* 2015; **10**:e0118564.

9 Carvajal RD, Sacco JJ, Jager MJ, Eschelman DJ, Olofsson Bagge R, Harbour JW *et al.* Advances in the clinical management of uveal melanoma. 2023.

10 Spagnolo F, Grosso M, Picasso V, Tornari E, Pesce M, Queirolo P. Treatment of metastatic uveal melanoma with intravenous fotemustine. *Melanoma Res* 2013; **23**:196–198.

11 Sacco JJ, Nathan PD, Danson S, Lorigan P, Nicholson S, Ottensmeier C, *et al.* Sunitinib versus dacarbazine as first-line treatment in patients with metastatic uveal melanoma. *J Clin Oncol* 2013; **31**:9031–9031.

12 Johansson P, Aoude LG, Wadt K, Glasson WJ, Warrier SK, Hewitt AW, *et al.* Deep sequencing of uveal melanoma identifies a recurrent mutation in PLCB4. *Oncotarget* 2016; **7**:4624–4631.

13 Moore AR, Ceraudo E, Sher JJ, Guan YX, Shoushtari AN, Chang MT, *et al.* Recurrent activating mutations of G-protein-coupled receptor CYSLTR2 in uveal melanoma. *Nat Genet* 2016; **48**:675–680.

14 Robertson AG, Shih J, Yau C, Gibb EA, Oba J, Mungall KL, *et al.*; TCGA Research Network. Integrative analysis identifies four molecular and clinical subsets in uveal melanoma. *Cancer Cell* 2017; **32**:204–220.e15.

15 Chen X, Wu Q, Tan L, Porter D, Jager MJ, Emery C, *et al.* Combined PKC and MEK inhibition in uveal melanoma with GNAQ and GNA11 mutations. *Oncogene* 2014; **33**:4724–4734.

16 Wu XQ, Li JJ, Zhu MJ, Fletcher JA, Hodi FS. Protein kinase C inhibitor AEB071 targets ocular melanoma harboring GNAQ mutations via effects on the PKC/Erk1/2 and PKC/NF-kappa B pathways. *Mol Cancer Ther* 2012; **11**:1905–1914.

17 Piperno-Neumann S, Kapiteijn E, Larkin JMG, Carvajal RD, Luke JJ, Seifert H, *et al.* Phase I dose-escalation study of the protein kinase C (PKC) inhibitor AEB071 in patients with metastatic uveal melanoma. *J Clin Oncol* 2014; **32**:9030–9030.

18 Kapiteijn E, Carlino M, Boni V, Loirat D, Speetjens F, Park J, *et al.* A Phase I trial of LXS196, a novel PKC inhibitor for metastatic uveal melanoma. *Cancer Res* 2019; **79**:CT068.

19 Vaque JP, Dorsam RT, Feng X, Iglesias-Bartolome R, Forsthoefel DJ, Chen Q, *et al.* A genome-wide RNAi screen reveals a Trio-regulated Rho GTPase circuitry transducing mitogenic signals initiated by G protein-coupled receptors. *Mol Cell* 2013; **49**:94–108.

20 Feng XD, Arang N, Rigiracciolo DC, Lee JS, Yeerna H, Wang ZY, *et al.* A platform of synthetic lethal gene interaction networks reveals that the GNAQ uveal melanoma oncogene controls the hippo pathway through FAK. *Cancer Cell* 2019; **35**:457–472.e5.

21 Feng XD, Degese MS, Iglesias-Bartolome R, Vaque JP, Molinolo AA, Rodrigues M, *et al.* Hippo-independent activation of YAP by the GNAQ uveal melanoma oncogene through a trio-regulated Rho GTPase signaling circuitry. *Cancer Cell* 2014; **25**:831–845.

22 Sorrentino G, Ruggeri N, Specchia V, Cordenonsi M, Mano M, Dupont S, *et al.* Metabolic control of YAP and TAZ by the mevalonate pathway. *Nat Cell Biol* 2014; **16**:357–366.

23 Nardone G, La Cruz JOD, Vrbsky J, Martini C, Pribyl J, Skladal P, *et al.* YAP regulates cell mechanics by controlling focal adhesion assembly. *Nat Commun* 2017; **8**:15321.

24 Genevet A, Tapon N. The Hippo pathway and apico-basal cell polarity. *Biochem J* 2011; **436**:213–224.

25 Gumbiner BM, Kim NG. The Hippo-YAP signaling pathway and contact inhibition of growth. *J Cell Sci* 2014; **127**:709–717.

26 Li HP, Li Q, Dang K, Ma S, Cotton JL, Yang S, *et al.* YAP/TAZ activation drives uveal melanoma initiation and progression. *Cell Rep* 2019; **29**:3200–3211.e4.

27 Yu FX, Luo J, Mo JS, Liu GB, Kim YC, Meng ZP, *et al.* Mutant Gq/11 promote uveal melanoma tumorigenesis by activating YAP. *Cancer Cell* 2014; **25**:822–830.

28 Crook ZR, Sevilla GP, Friend D, Brusniak MY, Bandaranayake AD, Clarke M, *et al.* Mammalian display screening of diverse cystine-dense peptides for difficult to drug targets. *Nat Commun* 2017; **8**:2244.

29 Luo MX, Xu YJ, Chen HF, Wu YQ, Pang A, Hu JJ, *et al.* Advances of targeting the YAP/TAZ-TEAD complex in the hippo pathway for the treatment of cancers. *Eur J Med Chem* 2022; **244**:114847.

30 Li LJ, Li RZ, Wang YM. Identification of small-molecule YAP-TEAD inhibitors by high-throughput docking for the treatment of colorectal cancer. *Bioorg Chem* 2022; **122**:105707.

31 Liu-Chittenden Y, Huang B, Shim JS, Chen Q, Lee SJ, Anders RA, *et al.* Genetic and pharmacological disruption of the TEAD-YAP complex suppresses the oncogenic activity of YAP. *Gene Dev* 2012; **26**:1300–1305.

32 Ma JF, Weng L, Bastian BC, Chen X. Functional characterization of uveal melanoma oncogenes. *Oncogene* 2021; **40**:806–820.

33 Kim YJ, Lee SC, Kim SE, Kim SH, Kim SK, Lee CS. YAP activity is not associated with survival of uveal melanoma patients and cell lines. *Sci Rep-Uk* 2020; **10**:6209.

34 Wang YM, Xu XY, Maglic D, Dill MT, Mojumdar K, Ng PKS, *et al.* Comprehensive molecular characterization of the hippo signaling pathway in cancer. *Cell Rep* 2018; **25**:1304–1317.e5.

35 Brouwer NJ, Konstantinou EK, Gragoudas ES, Marinkovic M, Luyten GPM, Kim IK, *et al.* Targeting the YAP/TAZ pathway in uveal and conjunctival melanoma with verteporfin. *Invest Ophth Vis Sci* 2021; **62**:3.

36 Wang H, Guo M, Wei H, Chen Y. Targeting MCL-1 in cancer: current status and perspectives. *J Hematol Oncol* 2021; **14**:67.

37 Sieghart W, Losert D, Strommer S, Cejka D, Schmid K, Rasoul-Rockenschaub S, *et al.* Mcl-1 overexpression in hepatocellular carcinoma: a potential target for antisense therapy. *J Hepatol* 2006; **44**:151–157.

38 Nakano T, Go T, Nakashima N, Liu D, Yokomise H. Overexpression of antiapoptotic MCL-1 predicts worse overall survival of patients with non-small cell lung cancer. *Anticancer Res* 2020; **40**:1007–1014.

39 Fofaria N, Frederick D, Sullivan R, Flaherty K, Srivastava S. Overexpression of Mcl-1 confers resistance to BRAFV600E inhibitors alone and in combination with MEK1/2 inhibitors in melanoma. *Oncotarget* 2015; **6**:40535–40556.

40 Wood K. Overcoming MCL-1-driven adaptive resistance to targeted therapies. *Nat Comm* 2020; **11**:531.

41 Bolomsky A, Vogler M, Cem Köse M, Heckman C, Ehx G, Ludwig H, *et al.* MCL-1 inhibitors, fast-lane development of a new class of anti-cancer agents. *J Hematol Oncol* 2020; **13**:173.

42 Ksander BR, Rubsamen PE, Olsen KR, Cousins SW, Streilein JW. Studies of tumor-infiltrating lymphocytes from a human choroidal melanoma. *Invest Ophth Vis Sci* 1991; **32**:3198–3208.

43 Chen PW, Murray TG, Uno T, Salgaller ML, Reddy R, Ksander BR. Expression of MAGE genes in ocular melanoma during progression from primary to metastatic disease. *Clin Exp Metastas* 1997; **15**:509–518.

44 Luyten GPM, Naus NC, Mooy CM, Hagemeijer A, KanMitchell J, VanDrunen E, *et al.* Establishment and characterization of primary and metastatic uveal melanoma cell lines. *Int J Cancer* 1996; **66**:380–387.

45 Amirouchene-Angelozzi N, Nemati F, Gentien D, Nicolas A, Dumont A, Carita G, *et al.* Establishment of novel cell lines recapitulating the genetic landscape of uveal melanoma and preclinical validation of mTOR as a therapeutic target. *Mol Oncol* 2014; **8**:1508–1520.

46 Herold MJ, van den Brandt J, Seibler J, Reichardt HM. Inducible and reversible gene silencing by stable integration of an shRNA-encoding lentivirus in transgenic rats. *P Natl Acad Sci USA* 2008; **105**:18507–18512.

47 Bliss CI. Calculation of microbial assays. *Bacteriol Rev* 1956; **20**:243–258.

48 Fitzgerald JB, Schoeberl B, Nielsen UB, Sorger PK. Systems biology and combination therapy in the quest for clinical efficacy. *Nat Chem Biol* 2006; **2**:458–466.

49 Borad MJ, Bai LY, Chen MH, Hubbard JM, Mody K, Rha SY, *et al*. Silmitasertib (CX-4945) in combination with gemcitabine and cisplatin as first-line treatment for patients with locally advanced or metastatic cholangiocarcinoma: a phase Ib/II study. *J Clin Oncol* 2021; **39**:312–312.

50 Andreeff M, Kelly KR, Yee K, Assouline S, Strair R, Popplewell L, *et al*. Results of the phase I trial of RG7112, a small-molecule MDM2 antagonist in leukemia. *Clin Cancer Res* 2016; **22**:868–876.

51 Vassilev LT, Vu BT, Graves B, Carvajal D, Podlaski F, Filipovic Z, *et al*. In vivo activation of the p53 pathway by small-molecule antagonists of MDM2. *Science* 2004; **303**:844–848.

52 O'Reilly T, McSheehy PMJ. Biomarker development for the clinical activity of the mTOR inhibitor everolimus (RAD001): processes, limitations, and further proposals. *Transl Oncol* 2010; **3**:65–79.

53 Garcia-Martinez JM, Moran J, Clarke RG, Gray A, Cosulich SC, Chresta CM, *et al*. Ku-0063794 is a specific inhibitor of the mammalian target of rapamycin (mTOR). *Biochem J* 2009; **421**:29–42.

54 Tripathy D, Bardia A, Sellers WR. Ribociclib (LEE011): mechanism of action and clinical impact of this selective cyclin-dependent kinase 4/6 inhibitor in various solid tumors. *Clin Cancer Res* 2017; **23**:3251–3262.

55 Rayson D, Lupichuk S, Potvin K, Dent S, Shenkier T, Dhesy-Thind S, *et al*. Canadian Cancer Trials Group IND197: a phase II study of foretinib in patients with estrogen receptor, progesterone receptor, and human epidermal growth factor receptor 2-negative recurrent or metastatic breast cancer. *Breast Cancer Res Tr* 2016; **157**:109–116.

56 Tse C, Shoemaker AR, Adickes J, Anderson MG, Chen J, Jin S, *et al*. ABT-263: a potent and orally bioavailable Bcl-2 family inhibitor. *Cancer Res* 2008; **68**:3421–3428.

57 Cang SD, Iragavarapu C, Savooji J, Song YP, Liu DL. ABT-199 (venetoclax) and BCL-2 inhibitors in clinical development. *J Hematol Oncol* 2015; **8**:129.

58 Kotschy A, Szlavik Z, Murray J, Davidson J, Maragno AL, Le Toumelin-Braizat G, *et al*. The MCL1 inhibitor S63845 is tolerable and effective in diverse cancer models. *Nature* 2016; **538**:477–482.

59 Szlavik Z, Csekei M, Paczal A, Szabo ZB, Sipos S, Radics G, *et al*. Discovery of S64315, a potent and selective Mcl-1 inhibitor. *J Med Chem* 2020; **63**:13762–13795.

60 Karasic TB, Chiorean EG, Sebti SM, O'Dwyer PJ. A phase I study of GGTI-2418 (geranylgeranyl transferase i inhibitor) in patients with advanced solid tumors. *Target Oncol* 2019; **14**:613–618.

61 Tron AE, Belmonte MA, Adam A, Aquila BM, Boise LH, Chiarparin E, *et al*. Discovery of Mcl-1-specific inhibitor AZD5991 and preclinical activity in multiple myeloma and acute myeloid leukemia. *Nat Commun* 2018; **9**:5341.

62 Noland CL, Gierke S, Schnier PD, Murray J, Sandoval WN, Sagolla M, *et al*. Palmitoylation of TEAD transcription factors is required for their stability and function in hippo pathway signaling. *Structure* 2016; **24**:179–186.

63 Chan P, Han X, Zheng BH, Deran M, Yu JZ, Jarugumilli GK, *et al*. Autopalmitoylation of TEAD proteins regulates transcriptional output of the Hippo pathway. *Nat Chem Biol* 2016; **12**:282–289.

64 Kaneda A, Seike T, Danjo T, Nakajima T, Otsubo N, Yamaguchi D, *et al*. The novel potent TEAD inhibitor, K-975, inhibits YAP1/TAZ-TEAD protein-protein interactions and exerts an anti-tumor effect on malignant pleural mesothelioma. *Am J Cancer Res* 2020; **10**:4399–4415.

65 Reggiani F, Gobbi G, Ciarrocchi A, Sancisi V. YAP and TAZ are not identical twins. *Trends Biochem Sci* 2021; **46**:154–168.

66 Zhao YL, Tyrishkin K, Sjaarda C, Khanal P, Stafford J, Rauh M, *et al*. A one-step tRNA-CRISPR system for genome-wide genetic interaction mapping in mammalian cells. *Sci Rep-Uk* 2019; **9**:14499.

67 Zanconato F, Forcato M, Battilana G, Azzolin L, Quaranta E, Bodega B, *et al*. Genome-wide association between YAP/TAZ/TEAD and AP-1 at enhancers drives oncogenic growth. *Nat Cell Biol* 2015; **17**:1218–1227.

68 Hong JH, Hwang ES, McManus MT, Amsterdam A, Tian Y, Kalmukova R, *et al*. TAZ, a transcriptional modulator of mesenchymal stem cell differentiation. *Science* 2005; **309**:1074–1078.

69 Murakami M, Tominaga J, Makita R, Uchijima Y, Kurihara Y, Nakagawa O, *et al*. Transcriptional activity of Pax3 is co-activated by TAZ. *Biochem Bioph Res Co* 2006; **339**:533–539.

70 Zanconato F, Battilana G, Forcato M, Filippi L, Azzolin L, Manfrin A, *et al*. Transcriptional addiction in cancer cells is mediated by YAP/TAZ through BRD4. *Nat Med* 2018; **24**:1599–1610.

71 Varelas X, Sakuma R, Samavarchi-Tehrani P, Peerani R, Rao BM, Dembowy J, *et al*. TAZ controls Smad nucleocytoplasmic shuttling and regulates human embryonic stem-cell self-renewal. *Nat Cell Biol* 2008; **10**:837–848.

72 Taniguchi K, Wu LW, Grivennikov SI, de Jong PR, Lian I, Yu FX, *et al*. A gp130-Src-YAP module links inflammation to epithelial regeneration. *Nature* 2015; **519**:57–62.

73 Yu FX, Zhao B, Panupinthu N, Jewell JL, Lian I, Wang LH, *et al*. Regulation of the hippo-YAP pathway by G-protein-coupled receptor signaling. *Cell* 2012; **150**:780–791.

74 Kim NG, Gumbiner BM. Adhesion to fibronectin regulates Hippo signaling via the FAK-Src-PI3K pathway. *J Cell Biol* 2015; **210**:503–515.

75 Serrano I, McDonald PC, Lock F, Muller WJ, Dedhar S. Inactivation of the Hippo tumour suppressor pathway by integrin-linked kinase. *Nat Commun* 2013; **4**:2976.

76 Dupont S, Morsut L, Aragona M, Enzo E, Giuletti S, Cordenonsi M, *et al*. Role of YAP/TAZ in mechanotransduction. *Nature* 2011; **474**:179–183.